Polyaniline/polyvinylpyrrolidone nanofibers via nozzle-free electrospinning

Received: 28 March 2023 | Revised: 3 August 2023 | Accepted: 8 August 2023

DOI: 10.1002/app.54586

RESEARCH ARTICLE

Applied Polymer SCIENCE WILEY

Polyaniline/polyvinylpyrrolidone nanofibers via nozzle-free electrospinning

Muhammad Waqas | **Francisco Javier Diaz Sanchez** | **Valentin C. Menzel** | **Ignacio Tudela** | **Norbert Radacsi** | **Dipa Ray** | **Vasileios Koutsos**

School of Engineering, Institute for Materials and Processes, The University of Edinburgh, Edinburgh, UK

Correspondence
Muhammad Waqas and Vasileios Koutsos, School of Engineering, Institute for Materials and Processes, The University of Edinburgh, Robert Stevenson Road, Edinburgh EH9 3FB, UK.
Email: muhammad.waqas@ed.ac.uk and vasileios.koutsos@ed.ac.uk

Funding information
Higher Education Commission, Pakistan

Abstract

Polyaniline (PANI) in its emeraldine base (PANI-EB) and salt (PANI-ES) forms was combined with polyvinylpyrrolidone (PVP) to produce nanofibers in a one-step electrospinning process using a nozzle-free electrospinning setup for the first time. The surface morphologies and chemical structure of the composite nanofibers were characterized by scanning electron microscopy (SEM), X-ray diffraction (XRD), Fourier transform infrared spectroscopy—attenuated total reflectance (FTIR-ATR), and energy-dispersive X-ray spectroscopy (EDX). Four PANI/PVP electrospun nanofibers with different PANI concentrations were prepared to investigate the effect of PANI concentration on the structure and properties of the nanofibers. The incorporation of different contents of PANI-EB and PANI-ES in the PVP solution and their impact on the fiber morphology were investigated.

KEYWORDS

conductive polymer electrospinning, nanofiber, nozzle-free electrospinning, PANI, polyaniline, PVP

1 | INTRODUCTION

Electrospinning is a versatile process used for producing fibers with diameters on the order of tens of nanometers to micrometers.[1–3] The one-dimensional (1D) and two-dimensional (2D) structured materials produced by electrospinning have attracted significant attention due to their ease of synthesis, promising properties, and possibilities of functionalization.[4] Polymer electrospun fibers have unique properties due to their high surface-to-volume ratio, fiber-length-to-diameter aspect ratio,[5] and porosity (generally ≥70%).[6] Nanofibers can be used for diverse applications such as filtration,[7] electronic textiles,[8,9] drug delivery,[5] tissue engineering,[10–12] wound dressing,[13] sensors,[14,15] and composites.[16]

The electrospinning process stimulates the electrified liquid jets to whip and elongate to form fine fibers. When a polymer solution is extruded through a nozzle-spinneret during conventional electrospinning, electrostatic forces that are induced by applying a high voltage cause a conical geometry known as the "Taylor cone" at the nozzle's orifice. The production output of needle-based electrospinning devices is typically low, ranging from 0.01 to 0.3 g/h,[17] so scaling up the process has been investigated increasingly as a viable option for industrializing the fabrication.[18,19] This has typically been accomplished over time by enlarging the spinneret's structure while maintaining an energetically secure and evenly distributed configuration.[17] Nozzle-free (free-surface) electrospinning is an alternative method that can produce fibers at high throughput without being constrained by a

clogged nozzle, as opposed to multi-nozzle electrospinning, which can result in inhomogeneous fibers because the electric field around a given nozzle is affected by the nearby jets.[20] Importantly, a lab-scaled high-throughput system can provide an economical alternative to industrially available upscaling equipment for nozzle-free electrospinning research.[19] In nozzle-free electrospinning, a rotating cylinder electrode works against a biased rotating collector electrode in a bath of polymer solution. The motor can be used to adjust the roller's rotational speed. Multiple Taylor cones emerge from the rotating electrode surface submerged in the solution bath when high-voltage power with a potential greater than 40 kV is applied between the two rotating electrodes. On the surface of the rotating spinneret, a significant number of Taylor cones are formed when voltage is applied to the roller, causing the liquid to change into a conical shape. It has been demonstrated that the nozzle-free electrospinning method is a reliable and effective way to create nanofibers.[9,19]

Intrinsically conducting polymers (ICPs) have drawn considerable attention because of their controllable electrical conductivity, ease of synthesis, low cost, magnetic, and optical properties.[21,22] A variety of conducting polymers (e.g., polypyrrole (PPY),[23] poly(p-phenylenevinylene) (PPV),[24] polyaniline (PANI),[8] poly(3,4-ethylene dioxythiophene) (PEDOT),[25] polythiophene (PTh),[26] and other derivatives, etc.), have unique electronic structures and properties conferring ICPs with high electrical conductivity, high electron affinity, and low ionization potentials. ICPs are organic polymers with controllable chemical and electrochemical properties, including reversible doping/dedoping.[27] Conducting polymer (CP) nanotubes, nanowires, and nanofibers can be produced using a variety of physical methods like electrospinning,[4] chemical methods like interfacial polymerization,[28] template-free method,[29] dilute polymerization,[30] reverse emulsion polymerization,[31] etc., and different lithography techniques.[32] Among each established technique, large scale production with controllable morphologies can only be produced using electrospinning. Numerous publications have shown that these conducting polymer nanostructures are promising materials for making polymeric nano-devices like chemical and biosensors, field-effect transistors, field emission and electrochromic display devices, super-capacitors, biocompatibility etc., and that they have clear advantages over their bulk counterparts in many types of applications.[33,34]

PANI has significant advantages among conducting polymers, such as it is based upon a low-cost aniline monomer, ease of synthesis, tunable electrical conductivity, and high environmental stability.[35] Conducting polymer electrospun mats provide the possibility of electrical conductivity while having a three-dimensional (3D) network of fibers. These electrospun nanofibers have higher porosity, higher surface area, and enhanced surface functionalities than the original material or any other known form of the material.[36,37]

PANI's electrospinning produces nanofiber-based nonwoven composite with attractive features and enhanced properties compared to the bulk material. PANI has a low molecular weight, low solubility, infusible nature, and rigid backbone structure, which makes it necessary to be blended with other nonconducting electrospinnable polymers to produce nanofibers. PANI exists in three isolable oxidation states, fully reduced leucoemeraldine base (LE), half oxidized/ half reduced emeraldine base (EB), and fully oxidized pernigraniline (PE). The conducting form of polyaniline emeraldine salt (PANI-ES) is produced by doping of polyaniline emeraldine base (PANI-EB) with protonic acids[38] and then blended with other polymers to be electrospun.[39] Many researchers have reported the electrospinning of blends containing a mixture of PANI and other polymers such as polyvinylpyrrolidone (PVP),[8] polystyrene,[40] polyacrylonitrile (PAN),[41] polyvinylidene fluoride (PVDF),[37,42] and polyethylene glycol (PEO).[43]

Polyvinylpyrrolidone (PVP) is a water-soluble polymer that has stability, a higher degree of compatibility with other polymers on a molecular level, and high mechanical strength.[44] It can be thermally cross-linked and can produce thermally stable blends.[45] It imparts properties such as high hardness, high crystallinity, low solubility, and thermal resistance to blends.[46] PVP is used as a steric stabilizer to intercept the agglomeration of colloids.[47] PANI and PVP blends are of particular interest because they exhibit the electrical properties of PANI and the mechanical properties of PVP.[48] In PANI/PVP polymer blends, a hydrogen bonding develops between the carbonyl group of PVP and nitrogen-hydrogen of PANI, which is responsible for PANI's dispersion in the blend.[49]

Doped PANI usage in polymer blend solutions has been reported extensively in the literature.[8,14,21,26,35,37,42,46,50–53] Much of the current literature presents varying results on the electrospun materials' enhanced electrical conductivity based on the doped PANI. There are several disadvantages associated with the use of doped PANI as compared to using pure PANI. First, the solution blend process is more prolonged, requiring several steps to get enough conductive PANI-ES. The filtration of doped PANI is usually needed before it is used in an electrospinning solution, which makes the estimation of PANI's actual content in the final solution more difficult.[54]

Prior research on PANI/PVP composite nanofibers used doped,[8] chemically modified,[55–58] or filtered

PANI.[36,59] However, to the best of our knowledge, there are no studies published in the scientific literature concerning the development of electrospun composite fibers using PVP and undoped EB and ES forms of polyaniline. In this work, both PANI-EB and PANI-ES were blended with PVP, and electrospun composite nanofibers were produced using a nozzle-free electrospinning technique. No filtration on PANI/PVP solution or chemical modification of PANI/PVP electrospun blends has been performed. The study aimed to investigate the nozzle-free electrospun polyaniline emeraldine salt (PANI-ES) and polyaniline emeraldine base (PANI-EB)/Polyvinylpyrrolidone (PVP) blend fiber diameter, morphology, and structure.

2 | MATERIALS AND METHODS

2.1 | Materials

The aniline monomer (99%, Alfa), ammonium peroxydisulfate (APS) 98% $(NH_4)_2S_2O_8$, acetone (99.9%), NH_4OH (24%), hydrochloric acid (1 M HCl), sodium hypochlorite (5% NaOCl), potassium biiodate (KH $(IO_3)_2$) and *N*,*N*-dimethylformamide (DMF) were purchased from Aldrich. Polyvinylpyrrolidone (PVP, M_w 1,300,000 g mol^{-1}) was purchased from Alfa-Aesar (USA). All the chemicals were used without further purification.

2.2 | Preparation of polyaniline emeraldine base and emeraldine salt

The standard polyaniline emeraldine base (PANI-EB) was prepared using the procedure described in Reference 39. Aniline (5 g) dissolved in 75 mL of 1 M HCl and 25°C. Ammonium peroxydisulfate (12.4 g) was dissolved in 70 mL of 1 M HCl and kept at 25°C. The two solutions were mixed and allowed to stand at 25°C for 30 min. The reaction mixture was then filtered using a Buchner funnel and flask, and the residue was washed with 10 × 80 mL of acetone. The filter cake (PANI-ES) was stirred in ammonium hydroxide solution (100 mL, 24%) for 1 h before filtering and washing with 10 × 100 mL of acetone. This was followed by drying under a dynamic vacuum at 60°C for 48 h to give blue powder.

The conductive nanofibril polyaniline emeraldine salt (PANI-ES) was prepared using a method followed from Reference 38. Aniline (1 mL, 0.1 M) was dissolved in 100 mL of 1 M HCl at room temperature by magnetic stirring for 15 min. A 100 mL of potassium biiodate (KH $(IO_3)_2$) (0.012 mM) was added to the solution and magnetically stirred for 5 min. Then the hypochlorite (5 mL) was added to the solution and left for 20 min with no stirring. The resulting green suspension product was filtered in a Buchner funnel. It was then continuously washed with hydrochloric acid (1 M HCl) and acetone until the filtrate became colorless and then dried at 60°C in a dynamic vacuum oven overnight.

2.3 | Electrospinning of PANI/PVP nanofiber electrospun mat

The PVP solutions (15 wt% and 18 wt%) were prepared by dissolving 12 g PVP and 14.4 g (M_w = 1,300,000 g mol^{-1}) powder in 80 mL of DMF and stirred overnight at 700 rpm at room temperature. The PANI solution was then prepared by dissolving 0.5 or 1 g of PANI-EB and PANI-ES separately in 10 mL of DMF at room temperature under continuous stirring at 400 rpm, respectively. The PANI-EB and PANI-ES solutions were separately mixed with the 18 wt% PVP/DMF solution to prepare the master solution. The mixed solution was stirred for 60 min to form a solution with complete homogeneity. The composition of each electrospinning solution is mentioned in Table 1. The samples are denoted as EB-*x* and ES-*x*, where *x* represents the weight percentage per mL (mg mL^{-1}) of PANI-EB and PANI-ES, respectively.

All solutions were electrospun using the home built nozzle-free electrospinning setup as shown in Figure 1 and described in detail in Reference 19. The nozzle-free electrospinning setup consists of a spiral coil spinneret slowly rotating in a solution bath made of Teflon. High voltage was connected with the rotating coil spinneret, which was partially immersed in a solution bath. The collector was connected with the opposite charge to that of the spinneret. A total potential difference in the range of 40–60 kV DC was applied between the two rotating electrodes. As the coil spinneret slowly rotates, a thin film of the polymer solution forms on the upper side of the spinneret, allowing for the jetting of fibers from multiple Taylor cones formed on its surface.

Conditioned hot air is blown into the electrospinning device from two heating assemblies. The heating assemblies can maintain a relative humidity of 15%–30% and a temperature between 15 and 30°C. The distance between the collector and the spinneret electrode was 15 cm.

2.4 | Characterization

All samples were examined under a scanning electron microscope (JEOL JSM-IT100, JEOL Ltd., Japan) operating at an accelerating voltage of 10 kV. Each SEM sample was prepared by placing each of them on carbon

TABLE 1 The different investigated concentrations of PANI/PVP and the corresponding electrical conductivity of the solution and average fiber diameter.

Composition of electrospinning solution in DMF	Name of sample	The electrical conductivity of the solution (μS cm^{-1})	Average fiber diameter (nm)
150 mg mL^{-1} PVP	PVP-1	7.22	166 ± 58
180 mg mL^{-1} PVP	PVP-2	7.27	89 ± 15
5.55 mg mL^{-1} PANI-EB	PANI-EB-5/PVP	10.15	366 ± 220
11.11 mg mL^{-1} PANI-EB	PANI-EB-11/PVP	17.81	286 ± 136
5.55 mg mL^{-1} PANI-ES	PANI-ES-5/PVP	37.4	189 ± 61
11.11 mg mL^{-1} PANI-ES	PANI-ES-11/PVP	50.4	219 ± 57

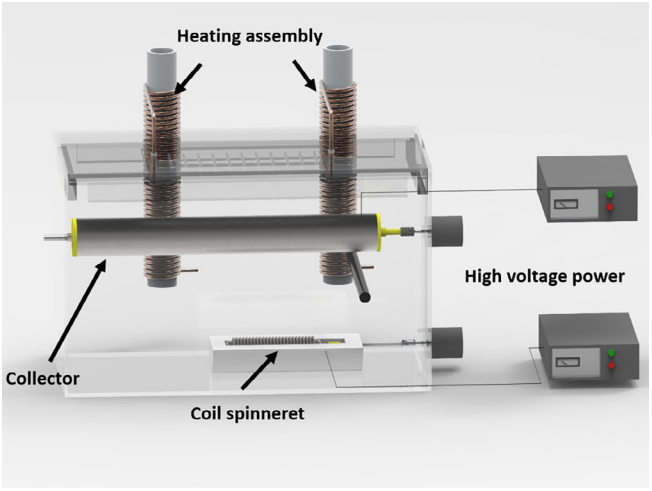

FIGURE 1 Nozzle-free electrospinning setup with a high voltage power source. A heating assembly was used for the conditioning of air. Nanofibers arise from a coil spinneret and are collected at a metallic collector. [Color figure can be viewed at wileyonlinelibrary.com]

conductive tape, which was attached to aluminum sample holders. Each sample was sputter-coated with a thin evaporated layer of gold, until reaching a thickness of approximately 100 Å using a sputter coater (AGB7341, Agar Scientific, UK). The fiber diameters were measured from the SEM images using the ImageJ software.[60] The fiber distribution was measured by selecting 50 fibers from the SEM images and the mean value with the standard deviation of the fiber diameter was reported. The EDX was performed on composite nanofibers using the Zeiss Crossbeam 550 focused ion beam SEM. The polyaniline dried powders were uniaxially pressed to produce pellets in a small hydraulic press. The diameter of the die was 13 mm, and 1-tonne force was applied for 3 min. The electrical conductivity of dry pressed polyaniline pellets was conducted employing the four point probe method using an Ossila four-point probe. The electrical conductivity of the electrospinning solution was measured with a portable Fisherbrand™ traceable conductivity measuring device by dipping the probe in the polymeric solution. The measured values of solution conductivity are shown in Table 1. The Bruker D2 PHASER X-ray diffraction (XRD) using Cu Kα X-rays of wavelength 1.54 Å was utilized to investigate the polyaniline crystallinity with a 5° per minute scan rate in the reflection mode over a range of 2θ from 0 to 60°. The Fourier transform infrared spectroscopy-attenuated total reflectance (FTIR-ATR) spectra (4000–400 cm^{-1}) of the samples were recorded using an FTIR-ATR spectrometer, Nicolet iS10. The FTIR-ATR spectrometer was used to confirm the presence of PANI/PVP-related functional groups and the chemical structure of the PANI. The baseline correction was made carefully using FTIR-ATR spectrometer software. All analysis of samples was performed without any additional sample preparation.

3 | RESULTS AND DISCUSSION

3.1 | Morphology and electrical conductivity of synthesized polyaniline

Chemical oxidative polymerization of aniline is the traditional method for preparing polyaniline. The typical fluffy granular powder morphology was observed for the PANI-EB polymer, Figure 2a. Polyaniline prepared using ammonium peroxydisulfate has a highly aggregated morphology. Angelopoulos et al. reported that PANI-EB tends to make inter-chain H-bonding between amine and imine sites resulting in aggregate formation.[61] Huang et al.[62] reported that oxidation of aniline is an exothermic reaction and in the early polymerization process, polyaniline nanofibers in the range of 30–50 nm are formed. When ammonium peroxydisulfate solution is added to aniline solution, after rapid sedimentation and aggregation the nanofibers become thickened and coarser, and the resulting structure comprises irregularly-shaped agglomerates.[28] Green-colored PANI-ES was synthesized

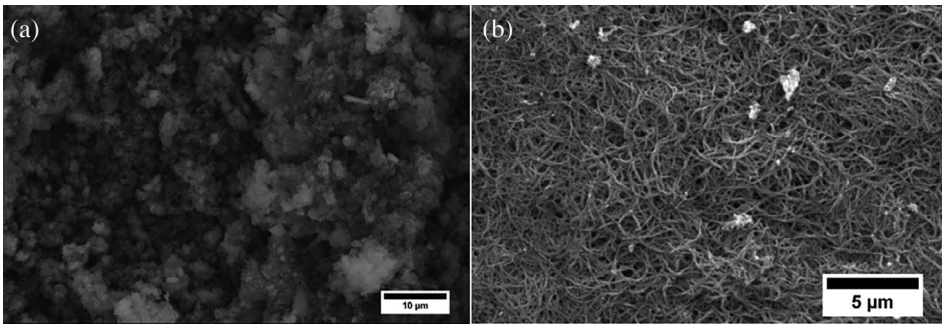

FIGURE 2 SEM micrograph of (a) polyaniline emeraldine base (PANI-EB) and (b) polyaniline emeraldine salt (PANI-ES).

after mixing aniline with two oxidants, potassium biiodate, and hypochlorite, in 1 M HCl solution. The SEM micrograph shown in Figure 2b demonstrates that the synthesized PANI-ES consists of an irregular mixture of fibrils and a few granular particles. The sodium hypochlorite's facilitates nanofiber growth and reduces nucleation site formation on the nanofiber surface.[63] Therefore, thinner and longer nanofibrils of PANI-ES were produced.

The bulk room temperature electrical conductivity of polyaniline pellets was measured using the four-point probe method. The electrical conductivity of PANI-EB is undetectable, outside of the range of the used Ossila four-point probe. Yilmaz et al. reported the electrical conductivity of PANI-EB in the order of magnitude of 10^{-3} S/cm.[39] The electrical conductivity of PANI-ES is 13.1 ± 1.71 S/cm which is ca. 7 times less than the value reported by Rahy et al.[38] Stejskal et al. reported that a 40% standard deviation in polyaniline's conductivity is possible for a set of polymerization even after following the same method.[64] Variable electrical conductivity could be caused by differences in reaction conditions, sample processing, and electrical measurement conditions, such as pellet size and pressure applied to a compressed pellet. The electrical conductivity of polyaniline can be greatly influenced by varying the different parameters of polymerization. To achieve maximum electrical conductivity it is very important to optimize the reaction speed, temperature, oxidant ratio, time of reaction, and acid ratio of PANI polymerization.[65] In addition to the above parameters, the diameter and length of the nanofibril structure of PANI-ES may have an influence on electrical conductivity. The average diameter and length of synthesized PANI-ES nanofibrils are 124 ± 24 nm, and 1.16 ± 0.28 µm, respectively, while Rahy et al. reported fibril average diameter and length of ca. 50 nm and 4 µm, respectively.

3.2 | X-ray diffraction analysis

The crystallinity and orientation of conducting polymers have been of much interest because more highly ordered

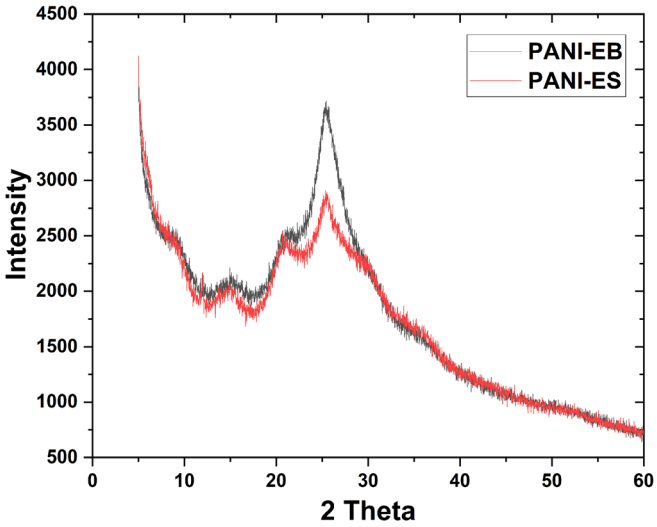

FIGURE 3 XRD graph of PANI-EB (black line) and PANI-ES (red line). [Color figure can be viewed at wileyonlinelibrary.com]

systems can display a metallic conductive state.[38] Many researchers reported that polyaniline has an X-ray diffraction pattern consisting of three peaks at 15°, 20°, and 25°.[63,66,67] Figure 3 shows that our sample also has three crystalline peaks, at ca. 15°, 20°, and 25°, which indicates that our sample has a crystalline nature. The characteristic peaks appeared at 15°, 20°, and 25°, corresponding to (011), (020), and (200) crystal planes of PANI.[28,65]

3.3 | Morphology of electrospun nanofibers composite

PVP, PANI-EB/PVP, and PANI-ES/PVP electrospun fiber composite were prepared employing nozzle-free electrospinning using varying fractions of PANI and PVP in the solution system. The composition of the electrospinning solution, the electrical conductivity of the solution, and the fiber diameter of PVP and PANI/PVP electrospun fibers are reported in Table 1. The average fiber diameters observed for the electrospun composite were measured from the SEM micrographs and determined by measuring

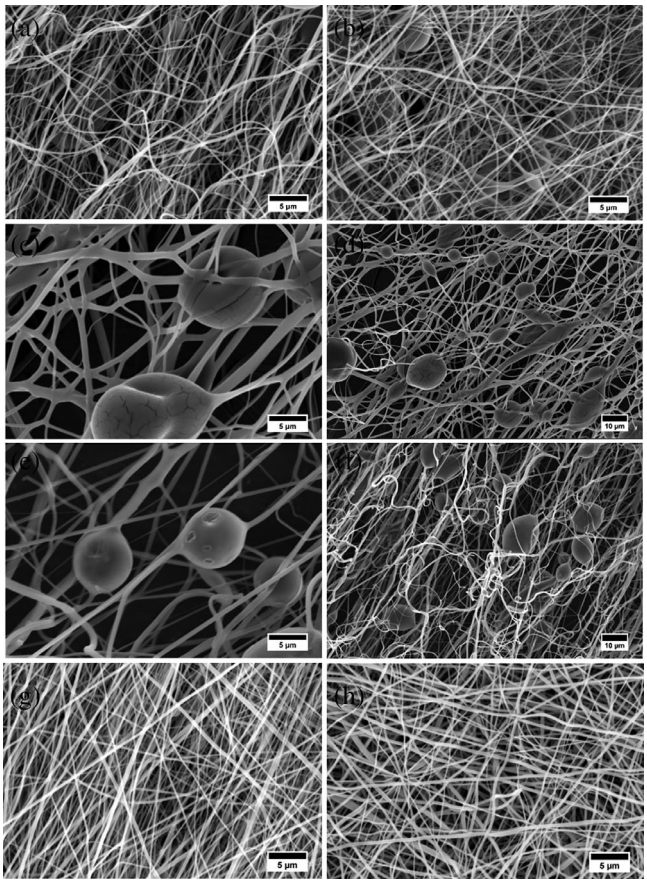

FIGURE 4 SEM images of (a) PVP-1, (b) PVP-2, (c, d) PANI-EB-5/PVP irregularly-shaped undissolved polymer particles are attached to nanofibers, (e, f) PANI-EB-11/PVP irregularly-shaped undissolved polymer particles are attached to nanofibers, (g) PANI-ES-5/PVP, and (h) PANI-ES-11/PVP.

the diameters of at least 50 random fibers. Two different forms: PANI-EB and PANI-ES were used with two different concentrations, 5.55 mg mL^{-1} and 11.11 mg mL^{-1} in the PANI/PVP electrospinning solution as given in Table 1. It has to be noted that blends containing more than 11.11 mg mL^{-1} PANI-ES were not suitable for electrospinning due to the high viscosity and high electrical conductivity of the solution.[37]

Figure 4 illustrates SEM images of the electrospun composite of PVP, PANI-EB/PVP, and PANI-ES/PVP. Histograms of the fiber diameter distributions and the average values for each case are presented in Figure 5. The electrospun fibers are randomly oriented fibrous networks. Figure 4a,b shows the electrospun fibers of pure PVP; with increasing the concentration of PVP, the average fiber diameter was also reduced from 166 ± 58 nm to 89 ± 15 nm. PVP was dissolved in DMF, which facilitates polymer dissolution by separating the ion pairs. Besides, its presence in the solution could raise the charge density and generate excessive charges, leading to nanofiber formation with smaller diameters.[68]

The morphology of PANI-EB/PVP electrospun fibers is shown in Figure 4c–f. The incorporation of PANI-EB in PVP solution resulted in an increase in electrospun fiber diameter to 366 ± 220 nm for PANI-EB-5/PVP Figure 4c,d, in agreement with the increase in PANI-EB/PVP electrospun fiber diameters with PANI-EB previously reported in the literature.[36] It is worth noting that the average fiber diameter of PANI-EB-5/PVP and PANI-EB-11/PVP electrospun fibers decreases from 366 ± 220 nm to 286 ± 136 nm, respectively with increasing PANI-EB content in the blend, as shown in Figure 5c,d. This behavior could be attributed to the difference in solution viscosity because of densely entangled polymer chains.[69] The reduction in fiber diameter is related to the high viscosity of the solution that prevents the jet from breaking up into droplets. Moreover, the increase in chain entanglements results in an increase in viscoelastic force, which can be enough to prevent the electrically charged jet's breakup.[20] As a result, the charged jet elongates toward the collector by Coulombic stress, and the diameter of the jet decreases.[69] As the PANI-EB content increases in the electrospinning solution, an increased presence of encapsulated micrometer-sized particles is detected attached within the PANI-EB/PVP fibers, as shown in the SEM images Figure 4c–f.[36] These particles might be undissolved PANI-EB, which remains in the solution system while electrospinning. Additional reasons for the encapsulation of PANI-EB particles might be the high surface tension of PANI molecules and the number of entanglements of PVP chains during the electrospinning process.[37,40] The presence of micro-sized porous particles of PANI-EB on the fiber surface results in an electrospun matrix with a higher surface area. The fibrous mat can be used to trap gaseous agents and might have higher surface interactions with polyaniline particles encapsulated within the electrospun mats.[53]

For the PANI-ES/PVP solution, with increasing PANI-ES content, the system electrical conductivity substantially increased, as mentioned in Table 1. The PANI-ES may affect the solution's electrical and viscoelastic properties by increasing its concentration in the solution.[50] The higher charge density and ionic conductivity can enhance the jet instability and higher splitting degree, making the overall electrospinning process challenging to control.[50] The potential difference of the applied voltage was adjusted from 40 kV to 60 kV during the electrospinning process to avoid the PANI-ES/PVP solutions electrospraying.

In contrast to PANI-EB/PVP, PANI-ES/PVP fibers display a different morphology. These nanofibers do not have any particles attached. This change in morphology might be attributed to the nano-sized fibrillar structure of

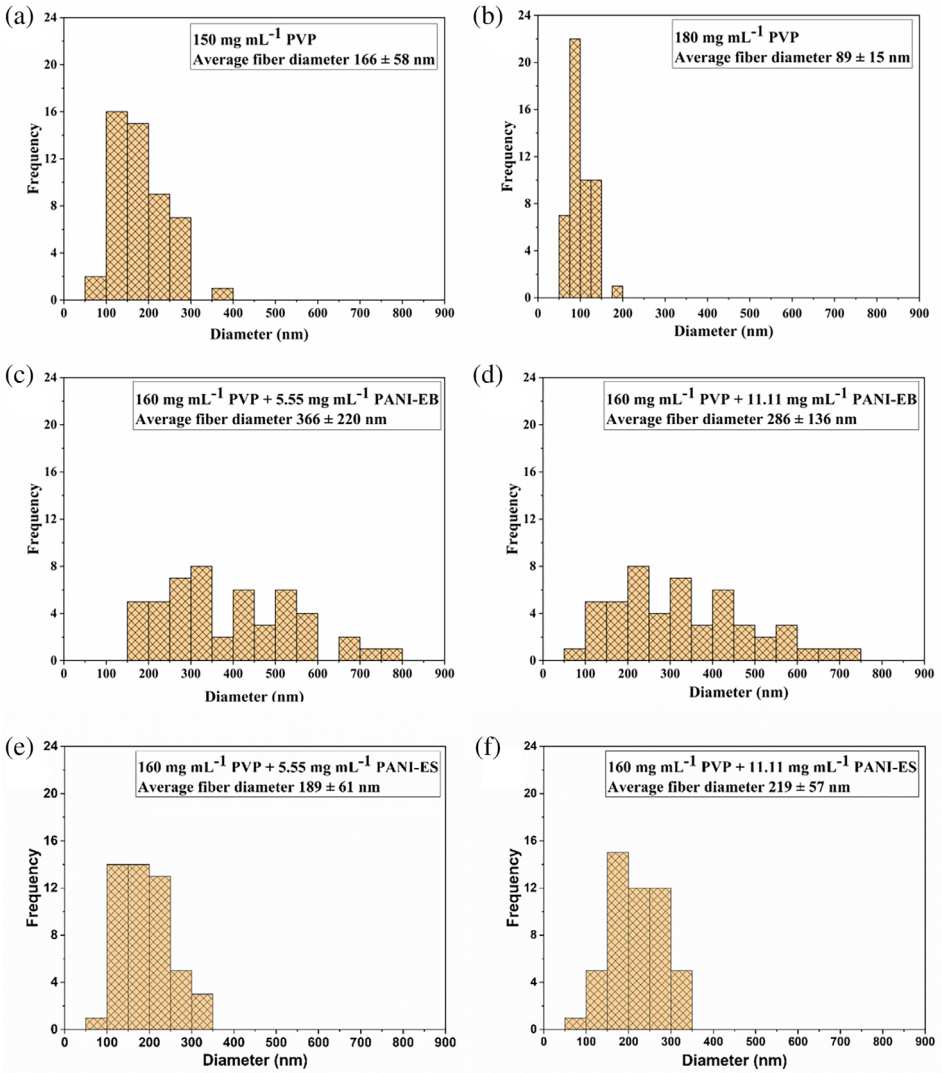

FIGURE 5 Histogram of the fiber diameters and average fiber diameters of electrospun composite (a) PVP-1, (b) PVP-2, (c) PANI-EB-5/PVP, (d) PANI-EB-11/PVP, (e) PANI-ES-5/PVP, and (f) PANI-ES-11/PVP. [Color figure can be viewed at wileyonlinelibrary.com]

PANI-ES, see Figure 2b. Colloidal stabilization can be achieved by electrostatic repulsion due to particle surface charge and/or steric repulsion (by the introduction of a polymer or a surfactant as stabilizer).[70] The backbone of the emeraldine form of polyaniline is positively charged by a protonic acid (H^+A^-). Therefore, a stable colloid could be formed through electrostatic repulsion without using a steric stabilizer if the particle size is very small or by steric repulsion via adsorbed PVP.[47,71]

The fiber morphology for PANI-ES-5/PVP and PANI-ES-11/PVP was smooth, uniform, and randomly oriented with a fiber diameter of 189 ± 61 nm and 219 ± 57 nm, respectively, see Figure 4g,h. As the amount of PANI-ES was increased from PANI-ES-5 to PANI-ES-11 in the PVP solution, a small increase in fiber diameters was observed, as presented in the histogram in Figure 5e,f. The polyaniline emeraldine salt content, viscosity, and strength of the electric field were the main parameters in determining the fiber diameters. The incorporation of salt increased the polymer jets stretching and reduced the incidence of bead formation by distributing the charges consistently to control the fiber uniformity.[35,72,73]

3.4 | FTIR-ATR of PANI and electrospun nanofibers

FTIR-ATR spectra of PANI-EB, PANI-ES, and PANI/PVP electrospun fibers are shown in Figure 6. The spectra of PANI-ES show two maxima bands of quinoid and benzenoid ring stretching vibrations at 1570 cm^{-1} and 1480 cm^{-1}, respectively. The band at 1243 cm^{-1} is C—$N^{+\cdot}$ stretching vibrations in the polaronic structure. The prominent band ~1136 cm^{-1} has been assigned to vibrations of the —NH^+═ structure.[36,74–76] FTIR spectra of PANI-EB powder demonstrate the vibrational bands groups at 824 cm^{-1} and 1141 cm^{-1}. The bands of quinoid and benzonoid ring vibrations were revealed at 1495 cm^{-1} and 1585 cm^{-1}. The peak at 1377 cm^{-1} was attributed to C—N stretching in the neighborhood of a

quinoid ring.[28,39,75,77] The PVP spectra show two main bands elongation of the accompanying OH is visible as a broadband at approximately 3400 cm^{-1}, and the strong band at 1644 cm^{-1} was also linked to the stretching vibrations of the free carbonyl groups in PVP. In addition, several bands are also seen in the range between 1245 and 1520 cm^{-1}. Both the band at 1443 cm^{-1} and the band at 1292 cm^{-1} are caused by the stretching of the molecules —(N—C)═O and —(C—N)—C, respectively.[78,79]

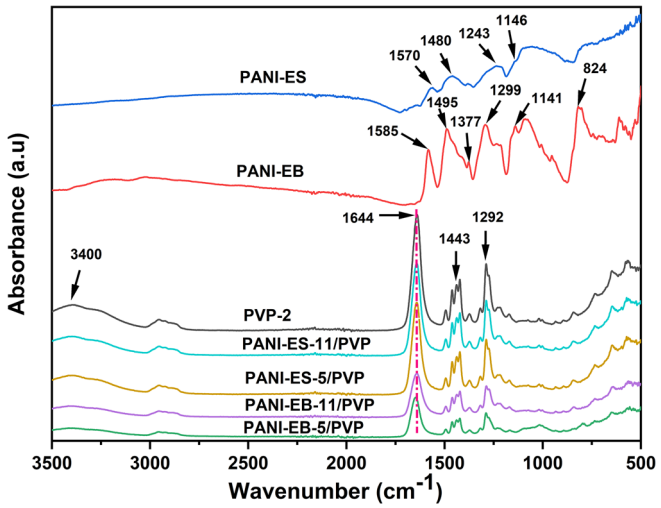

FIGURE 6 FTIR-ATR spectra of PANI-EB, PANI-ES powders, and PANI-PVP electrospun fibers in the 3500–500 cm^{-1} region. [Color figure can be viewed at wileyonlinelibrary.com]

The PVP and PANI/PVP nanofibers spectra are almost identical because higher concentrations of PVP are used to prepare the PANI/PVP electrospinning solution. The pure PVP nanofiber spectrum exhibits one characteristic band at 1644 cm^{-1}, which corresponds to free carbonyl, while the PANI powder spectra exhibit no absorptivity in the carbonyl region. In PANI/PVP nanofibers spectra, this band gradually shifted to a mode of lower frequency stretching. This shift can be attributed to a rise in the stiffness of PVP rings and may also be seen as proof of the existence of a hydrogen connection between PVP and PANI.[76,78]

3.5 | Elemental analysis of electrospun nanofibers

To identify the chemical composition of the particles attached to the PANI-EB/PVP nanofibers composite, an elemental analysis was carried out using Energy-Dispersive X-ray spectroscopy (EDX). Three different EDX spectra were obtained during the EDX analysis and are shown in Figure 7. Both PVP and PANI have C, H,

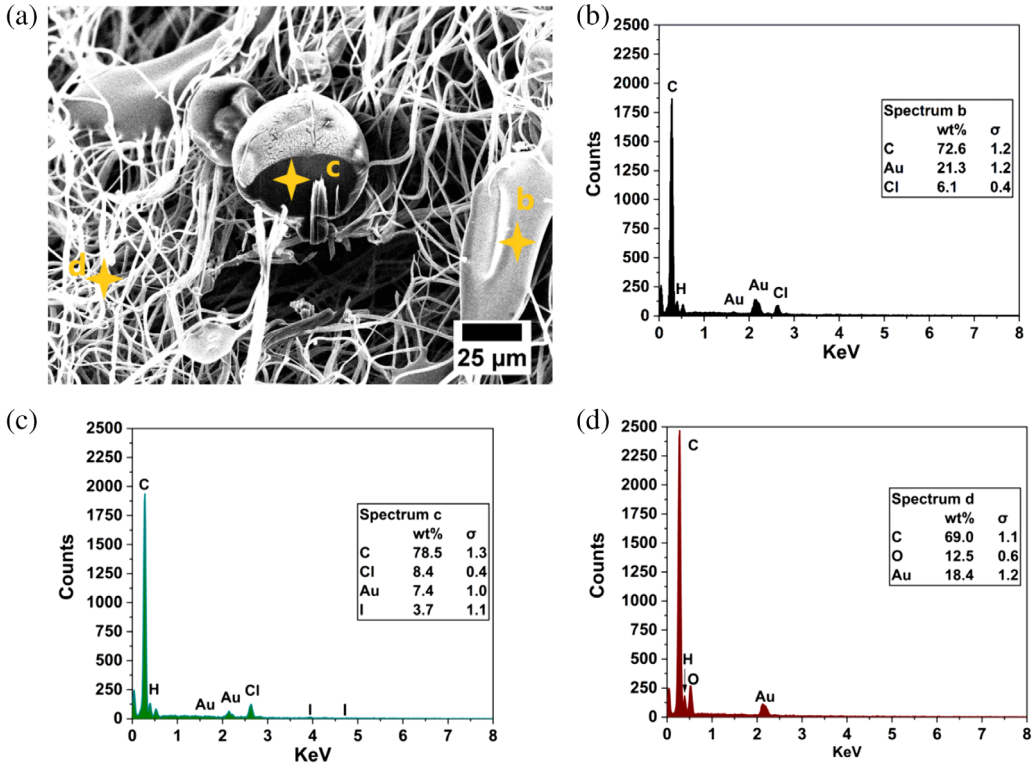

FIGURE 7 EDX analysis of PANI-EB-11/PVP (a) SEM image showing the positions b, c, and d (b–d) corresponding EDX spectra of PANI-EB-11/PVP corresponding to positions b, c, and d, respectively. [Color figure can be viewed at wileyonlinelibrary.com]

and N atoms in their chemical structures. PVP contains the O atom, whereas PANI does not. The EDX spectrum in Figure 7b on the irregular-shaped polymer particle at position b in Figure 7a shows the elements of carbon (C), chlorine (Cl), hydrogen (H), and gold (Au). The 6.1% amount of Cl proves that PANI was synthesized in an acidic medium (HCl).[39,80] The electrospun nanofibers were sputter-coated and this is the source of Au. A focused ion beam was used to cut an irregularly shaped polymer particle cross-sectionally (position c), and the EDX analysis was performed on that exposed surface. The spectrum at position c in Figure 7a presented in Figure 7c exhibits lower levels of Au, but matches closely the levels of C, H, and Cl shown in Figure 7b, providing further verification that these irregular particles are PANI-EB particles attached/incorporated to the electrospun fibers. However, the EDX spectrum at position d of Figure 7a on electrospun fibers shown in Figure 7d has peaks of C, H, and O, and the percentage of C is reduced to 69%, indicating that these are the PVP/PANI blend electrospun fibers.[39,56]

4 | CONCLUSIONS

In this work, polyaniline (PANI) in its emeraldine base (PANI-EB) and salt (PANI-ES) forms was combined with polyvinylpyrrolidone (PVP) to produce nanofibers in a one-step electrospinning process using a nozzle-free electrospinning setup. There has been no filtration of the PANI/PVP solution before electrospinning or any other chemical modification performed on PANI/PVP electrospun nanofibers. The different morphology of PANI-ES and PANI-EB affected the PANI/PVP solution properties and influenced the electrospinning process, morphology, and diameters of the electrospun nanofibers. The electrospinning of the PANI-EB/PVP solution is easy to perform compared to the solution containing PANI-ES because the addition of PANI-ES changes the solution's ionic conductivity. A higher voltage was applied for PANI-ES/PVP solutions during electrospinning to avoid electrospraying, which resulted in slightly thinner nanofibers. The PANI-ES/PVP electrospun fibers are well formed, smooth, and uniform exhibiting diameters of ca. 200 ± 60 nm. The PANI-EB/PVP nanofibers have PANI-EB irregularly shaped microparticles attached to the fibers, which are discontinuous and randomly oriented. However, similar fiber morphology was not observed for PANI-ES/PVP electrospun fibers due to the nanofibril morphology of PANI-ES. The higher surface area of PANI/PVP electrospun nanofibers and encapsulation of PANI-EB particles around nanofibers make them promising materials for gas sensing, filtration, biocompatibility, and membrane applications.

AUTHOR CONTRIBUTIONS

Muhammad Waqas: Data curation (lead); formal analysis (lead); funding acquisition (lead); investigation (lead); methodology (lead); validation (lead); visualization (lead); writing – original draft (lead); writing – review and editing (lead). **Francisco Javier Diaz Sanchez:** Data curation (supporting); investigation (supporting); writing – review and editing (supporting). **Valentin C. Menzel:** Data curation (supporting); writing – review and editing (supporting). **Ignacio Tudela:** Data curation (supporting); formal analysis (supporting); resources (supporting); writing – review and editing (supporting). **Norbert Radacsi:** Conceptualization (equal); data curation (supporting); formal analysis (supporting); investigation (supporting); methodology (supporting); project administration (supporting); resources (supporting); supervision (equal); writing – review and editing (supporting). **Dipa Ray:** Conceptualization (supporting); investigation (supporting); methodology (supporting); supervision (supporting); writing – review and editing (supporting). **Vasileios Koutsos:** Conceptualization (lead); formal analysis (lead); investigation (supporting); methodology (lead); project administration (lead); resources (lead); supervision (lead); writing – original draft (supporting); writing – review and editing (supporting).

ACKNOWLEDGMENTS

The first author would like to thank the Higher Education Commission (HEC), Pakistan for their financial support. Additionally, the authors extend their thanks to Fergus Dingwall for his valuable assistance during the synthesis of polyaniline, and Dr. Gary Nichol for his support with XRD characterization. Miss. Katalin Kis is also acknowledged for her valuable support with FTIR-ATR characterization. The authors acknowledge using the Cryo FIB-SEM bought with the EPSRC grant EP/P03 0564/1, and express thanks to Dr. Thomas Glen for help with EDX analysis. For the purpose of open access, the author has applied a Creative Commons Attribution (CC BY) license to any author accepted manuscript version arising from this submission.

CONFLICT OF INTEREST STATEMENT

The authors declare no conflict of interest.

DATA AVAILABILITY STATEMENT

The data that support the findings of this study are available from the corresponding author upon reasonable request.

ORCID

Muhammad Waqas https://orcid.org/0000-0002-1251-0492

Vasileios Koutsos https://orcid.org/0000-0002-2203-8179

REFERENCES

[1] A. Formhals, *Process and apparatus for preparing artificial threads*. US 1,975,504. **1934**.

[2] O. Jirsak, F. Sanetrnik, D. Lukas, V. Kotek, L. Martinova, J. Chaloupek, *Method of nanofibres production from a polymer solution using electrostatic spinning and a device for carrying out the method*, Google Patents. **2009**.

[3] Y. Li, J. Zhu, H. Cheng, G. Li, H. Cho, M. Jiang, Q. Gao, X. Zhang, *Adv. Mater. Technol.* **2021**, *6*, 2100410.

[4] N. Radacsi, F. D. Campos, C. R. I. Chisholm, K. P. Giapis, *Nat. Commun.* **2018**, *9*, 4740.

[5] C. Cleeton, A. Keirouz, X. Chen, N. Radacsi, *ACS Biomater. Sci. Eng.* **2019**, *5*, 4183.

[6] A. Thorvaldsson, H. Stenhamre, P. Gatenholm, P. Walkenström, *Biomacromolecules* **2008**, *9*, 1044.

[7] X. Qin, S. Subianto, *Electrospun Nanofibers*, Woodhead Publishing, Duxford, UK **2017**, p. 449.

[8] P. Perdigão, B. M. M. Faustino, J. Faria, J. P. Canejo, J. P. Borges, I. Ferreira, A. C. Baptista, *Fibers* **2020**, *8*, 24.

[9] F. J. D. Sanchez, M. Chung, M. Waqas, V. Koutsos, S. Smith, N. Radacsi, *Nano Energy* **2022**, *98*, 107286.

[10] A. Keirouz, M. Zakharova, J. Kwon, C. Robert, V. Koutsos, A. Callanan, X. Chen, G. Fortunato, N. Radacsi, *Mater. Sci. Eng. C* **2020**, *112*, 110939.

[11] F. Fazal, F. J. D. Sanchez, M. Waqas, V. Koutsos, A. Callanan, N. Radacsi, *Med. Eng. Phys.* **2021**, *94*, 52.

[12] F. Fazal, F. P. W. Melchels, A. McCormack, A. F. Silva, A. Callanan, V. Koutsos, N. Radacsi, *J. Mech. Behav. Biomed. Mater.* **2023**, *139*, 105665.

[13] A. Keirouz, N. Radacsi, Q. Ren, A. Dommann, G. Beldi, K. Maniura-Weber, R. M. Rossi, G. Fortunato, *J. Nanobiotechnol.* **2020**, *18*, 51.

[14] N. Amariei, L. R. Manea, A. P. Bertea, R. Cramariuc, A. Bertea, O. Cramariuc, *IOP Conf. Ser.: Mater. Sci. Eng.* **2017**, *209*, 012091.

[15] H. Souri, H. Banerjee, A. Jusufi, N. Radacsi, A. A. Stokes, I. Park, M. Sitti, M. Amjadi, *Adv. Intell. Syst.* **2020**, *2*, 2000039.

[16] A. Dodero, M. Alloisio, S. Vicini, M. Castellano, *Carbohydr. Polym.* **2020**, *227*, 115371.

[17] H. Niu, T. Lin, *J. Nanomater.* **2012**, *2012*, 12.

[18] S. Omer, L. Forgách, R. Zelkó, I. Sebe, *Pharmaceutics* **2021**, *13*, 286.

[19] M. Waqas, A. Keirouz, M. K. S. Putri, F. Fazal, F. J. D. Sanchez, D. Ray, V. Koutsos, N. Radacsi, *Med. Eng. Phys.* **2021**, *92*, 80.

[20] A. M. Gañán-Calvo, *Phys. Rev. Lett.* **1997**, *79*, 217.

[21] M. Yanılmaz, A. Sezai Sarac, *Text. Res. J.* **2014**, *84*, 1325.

[22] T. K. Das, S. Prusty, *Polym. Plast. Technol. Eng.* **2012**, *51*, 1487.

[23] L. P. Júnior, D. B. R. D. S. Silva, M. F. de Aguiar, *J. Mol. Liq.* **2019**, *275*, 452.

[24] H. Okuzaki, *Macromolecules* **2006**, *39*, 4276.

[25] J. Cárdenas-Martínez, B. L. España-Sánchez, R. Esparza, J. A. Ávila-Niño, *Synth. Met.* **2020**, *267*, 116436.

[26] W. Matysiak, T. Tański, W. Smok, K. Gołombek, E. Schab-Balcerzak, *Appl. Surf. Sci.* **2020**, *509*, 145068.

[27] N. P. S. Chauhan, M. Mozafari, *Fundamentals and Emerging Applications of Polyaniline*, Elsevier, Amsterdam, Netherlands **2019**, p. 1.

[28] A. Abdolahi, E. Hamzah, Z. Ibrahim, S. Hashim, *Materials* **2012**, *5*, 1487.

[29] H. Ding, J. Shen, M. Wan, Z. Chen, *Macromol. Chem. Phys.* **2008**, *209*, 864.

[30] N. R. Chiou, A. J. Epstein, *Adv. Mater.* **2005**, *17*, 1679.

[31] S. Palaniappan, A. Joh, *Prog. Polym. Sci.* **2008**, *33*, 732.

[32] C. Huang, B. Dong, L. Nan, B. Yang, L. Liguo Gao, D. Q. Tian, W. Qiong, L. Chi, *Small* **2009**, *5*, 583.

[33] Y.-Z. Long, M.-M. Li, G. Changzhi, M. Wan, J.-L. Duvail, Z. Liu, Z. Fan, *Prog. Polym. Sci.* **2011**, *36*, 1415.

[34] X. Lu, W. Zhang, C. Wang, T.-C. Wen, Y. Wei, *Prog. Polym. Sci.* **2011**, *36*, 671.

[35] S. I. Abd Razak, I. F. Wahab, F. Fadil, F. N. Dahli, A. Z. Md Khudzari, H. Adeli, *Adv. Mater. Sci. Eng.* **2015**, *2015*, 1.

[36] J. C.-C. Wu, S. Ray, M. Gizdavic-Nikolaidis, J. Jin, R. P. Cooney, *Synth. Met.* **2016**, *217*, 202.

[37] C. Merlini, A. Pegoretti, T. M. Araujo, S. D. A. S. Ramoa, W. H. Schreiner, G. M. de Oliveira Barra, *Synth. Met.* **2016**, *213*, 34.

[38] A. Rahy, D. J. Yang, *Mater. Lett.* **2008**, *62*, 4311.

[39] F. Yılmaz, Z. Küçükyavuz, *e-Polymers* **2009**, *9*, 5.

[40] M. Wei, J. Lee, B. Kang, J. Mead, *Macromol. Rapid Commun.* **2005**, *26*, 1127.

[41] P. Heikkilä, A. Harlin, *Polym. Lett.* **2009**, *3*, 437.

[42] C. Merlini, G. M. O. Barra, T. Medeiros Araujo, A. Pegoretti, *RSC Adv.* **2014**, *4*, 15749.

[43] P. Moutsatsou, K. Coopman, M. B. Smith, S. Georgiadou, *Polymer* **2015**, *77*, 143.

[44] M. Y. Kariduraganavar, A. A. Kittur, R. R. Kamble, in *Natural and Synthetic Biomedical Polymers* (Eds: S. G. Kumbar, C. T. Laurencin, M. Deng), Elsevier, Oxford **2014**, p. 1.

[45] W. S. Khan, N. N. Hamadneh, W. A. Khan, *PLoS One* **2017**, *12*, e0183920.

[46] E. M. Abdelrazek, H. M. Ragab, M. Abdelaziz, *Plast. Polym. Technol.* **2013**, *2*, 1.

[47] D. Li, R. B. Kaner, *Chem. Commun.* **2005**, *26*, 3286.

[48] M. T. Taghizadeh, S. Nasirianfar, *Polym. Plast. Technol. Eng.* **2018**, *57*, 1893.

[49] E. Subramanian, G. Anitha, N. Vijayakumar, *J. Appl. Polym. Sci.* **2007**, *106*, 673.

[50] N. Meng, X. Wang, B. Xin, Z. Chen, Y. Liu, *Text. Res. J.* **2018**, *89*, 2490.

[51] J. P. F. Santos, M. Arjmand, G. H. F. Melo, K. Chizari, R. E. S. Bretas, U. Sundarara, *Mater. Des.* **2018**, *141*, 333.

[52] Y. Zhang, G. C. Rutledge, *Macromolecules* **2012**, *45*, 4238.

[53] V. C. Menzel, I. Tudela, *Curr. Opin. Chem. Eng.* **2022**, *35*, 100742.

[54] N. Savest, T. Plamus, K. Kütt, U. Kallavus, M. Viirsalu, E. Tarasova, V. Vassiljeva, I. Krasnou, A. Krumme, *J. Electrostat.* **2018**, *96*, 40.

[55] A. Bishop, P. Gouma, *Rev. Adv. Mater. Sci.* **2005**, *10*, 209.

[56] W. Liu, T. Zhong, T. Liu, J. Zhang, H. Liu, *ACS Appl. Polym. Mater.* **2020**, *2*, 2819.

[57] W. Liu, J. Zhang, H. Liu, *Polymer* **2019**, *11*, 954.

[58] A. Macagnano, E. Zampetti, S. Pantalei, F. De Cesare, A. Bearzotti, K. C. Persaud, *Thin Solid Films* **2011**, *520*, 978.

[59] A. Sidek, R. Arsat, X. He, K. Kalantar-Zadeh, W. Wlodarski, *Presented at 2012 International Conference on Enabling Science and Nanotechnology*, Johor Bahru, Malaysia, January **2012**.

[60] C. A. Schneider, W. S. Rasband, K. W. Eliceiri, *Nat. Methods* **2012**, *9*, 671.
[61] M. Angelopoulos, R. Dipietro, W. G. Zheng, A. G. MacDiarmid, A. J. Epstem, *Synth. Met.* **1997**, *84*, 35.
[62] J. Huang, R. B. Kaner, *Chem. Commun.* **2006**, *4*, 367.
[63] A. Rahy, M. Sakrout, S. Manohar, S. J. Cho, J. Ferraris, D. J. Yang, *Chem. Mater.* **2008**, *20*, 4808.
[64] J. Stejskal, R. G. Gilbert, *Pure Appl. Chem.* **2002**, *74*, 857.
[65] S. Kamarudin, M. S. A. Rani, M. Mohammad, N. H. Mohammed, M. S. Su'ait, M. A. Ibrahim, N. Asim, H. Razali, *J. Mater. Res. Technol.* **2021**, *14*, 255.
[66] K. Lee, S. Cho, S. H. Park, A. J. Heeger, C.-W. Lee, S.-H. Lee, *Nature* **2006**, *441*, 65.
[67] C.-H. Chen, *Appl. Polym. Sci.* **2003**, *89*, 2142.
[68] Q. Yang, Z. Li, Y. Hong, Y. Zhao, S. Qiu, C. E. Wang, Y. Wei, *J. Polym. Sci. B: Polym. Phys.* **2004**, *42*, 3721.
[69] F. Yalcinkaya, B. Yalcinkaya, O. Jirsak, *Electrospinning – Material, Techniques, and Biomedical Applications*, IntechOpen, London, UK **2016**.
[70] R. J. Hunter, *Foundations of Colloid Science*, Oxford University Press, Oxford, UK **2001**.
[71] Y.-Y. Wang, W.-J. Sun, H. Lin, P.-P. Gao, J.-F. Gao, K. Dai, D.-X. Yan, Z.-M. Li, *Composites B: Eng.* **2020**, *199*, 108309.
[72] F. Raeesi, M. Nouri, A. K. Haghi, *e-Polymers* **2009**, *9*, 114.
[73] P. Sengupta, A. Ghosh, N. Bose, S. Mukherjee, A. R. Chowdhury, P. Datta, *J. Appl. Polym. Sci.* **2020**, *137*, 49115.
[74] M. Radoičić, Z. Šaponjić, J. Nedeljković, G. Ćirić-Marjanović, J. Stejskal, *Synth. Met.* **2010**, *160*, 1325.
[75] D. Nuzhnyy, J. Petzelt, I. Rychetský, M. Trchová, J. Stejskal, *Synth. Met.* **2015**, *209*, 561.
[76] Y. Zhang, Y. Duan, J. Liu, G. Ma, M. Huang, *J. Phys. Chem. C* **2018**, *122*, 2032.
[77] N. V. Blinova, J. Stejskal, M. Trchová, J. Prokeš, *Polymer* **2006**, *47*, 42.
[78] S. Atia, K. Zeggagh, S. Hadjout, A. Etxeberria, Z. Benabdelghani, *J. Polym. Res.* **2022**, *29*, 138.
[79] S. W. Kuo, F. C. Chang, *Macromolecules* **2001**, *34*, 5224.
[80] J. Molina, M. F. Esteves, J. Fernández, J. Bonastre, F. Cases, *Eur. Polym. J.* **2011**, *47*, 2003.

How to cite this article: M. Waqas, F. J. D. Sanchez, V. C. Menzel, I. Tudela, N. Radacsi, D. Ray, V. Koutsos, *J. Appl. Polym. Sci.* **2023**, e54586. https://doi.org/10.1002/app.54586